An Experimental Study of the Influence of Eccentricity on Shear Lag Effects in Welded Connections

KENNETH L. ORLOFF, JAMES A. SWANSON, GIAN ANDREA RASSATI, and THOMAS M. BURNS

ABSTRACT

In the 2010 AISC *Specification*, the shear lag factor for longitudinally welded tension members was applicable only to plate-type members having equal length welds on each side with a minimum length equal to the distance between the welds (AISC, 2010). Fortney and Thornton (2012) used experimental data from three previous research programs consisting of 175 various tension members to develop a generalized shear lag model that addresses the aforementioned limitations. The members comprising this dataset consisted of 158 flat plates with equal weld lengths, 4 single angles with unequal but balanced weld lengths, and 13 other members having equal weld lengths. The shear lag factor presented in the 2016 AISC *Specification* Table D3.1, Case 4 (AISC, 2016b) is a product of Fortney and Thornton's work and applies to longitudinally welded plates, angles, channels, tees, and W-shapes having equal or unequal lengths and no length-to-width limitation. This paper presents an experimental study on the shear lag effects in longitudinally welded tension members under both in-plane and out-of-plane eccentricity through the testing of eight 3×½ plate sections and twelve 3×3×½ single-angle sections having both equal and unequal longitudinal weld lengths. Experimental shear lag factors were determined for each of the 20 tested specimens and compared to three theoretical values: (1) the shear lag factor in the 2010 AISC *Specification* (AISC, 2010), (2) the shear lag factor based on a bi-planar model (Fortney and Thornton, 2012), and (3) the shear lag factor from Case 4 in the 2016 AISC *Specification*. The findings of this experimental study confirm that shear lag factor given by Case 4 in the 2016 AISC *Specification* provides the best prediction of shear lag factors in welded connections subject to both in-plane and out-of-plane eccentricity.

KEYWORDS: Shear lag, angle, eccentric, tension member.

INTRODUCTION

Tension members are an efficient way to transfer stress from one point to another in a structure and are commonly found in bridge and roof trusses, wind bracing systems in buildings, cables in bridges, and rods in suspended roof systems. In order to successfully transfer stress from one member to another, tension members must be adequately connected using bolts or welds. Should the bolts or welds have sufficient strength, there are three limit states that may control the strength of a tension member: yielding of the gross section, fracture of the net section at the connection, and block shear fracture at the connection (Salmon et al., 2009). Gross section yielding is considered a limit state because it could lead to excessive elongation of the member while net section fracture and block shear fracture are considered limit states because the member would no longer be able to carry load. Net section fracture of a welded connection depends on the cross-sectional element being used as the tension member and on the connection details.

The design provisions for longitudinally welded tension members are located in Chapter D of the 2016 *Specification for Structural Steel Buildings* (AISC, 2016b), hereafter referred to as the AISC *Specification*. The design tensile strength, ϕP_n, and the allowable tensile strength, P_n/Ω, of a tension member is the lower value obtained when considering the limit states of tensile yielding in the gross section and tensile rupture in the net section. The nominal tensile strength of a tension member is as follows:

For tensile yielding in the gross section, the nominal tensile strength is:

$$P_n = F_y A_g \tag{1}$$

For tensile rupture in the net section, the nominal tensile strength is:

$$P_n = F_u A_e \tag{2}$$

The effective net area of the tension member, A_e, is determined as:

$$A_e = A_n U \tag{3}$$

Kenneth L. Orloff, The Dwyer Company Inc., Cincinnati, Ohio. Email: korloff@thedwyercompany.com

James A. Swanson, Associate Professor, Department of Civil and Architectural Engineering and Construction Management, University of Cincinnati, Cincinnati, Ohio. Email: james.swanson@uc.edu (corresponding)

Gian Andrea Rassati, Associate Professor, Department of Civil and Architectural Engineering and Construction Management, University of Cincinnati, Cincinnati, Ohio. Email: gian.rassati@uc.edu

Thomas M. Burns, Adjunct Professor, Department of Civil and Architectural Engineering and Construction Management, University of Cincinnati, Cincinnati, Ohio. Email: burnstm@ucmail.uc.edu

Paper No. 2019-01

where

A_g = gross area of the member, in.^{2}
A_n = net area of the member, in.^{2}
U = shear lag reduction coefficient

AISC *Specification* Table D3.1 provides shear lag factors for various cases. Because this experimental study focused on the effect that eccentricity has on shear lag factors, Case 4 as listed in the table is of prime interest, as shown in Figure 1.

BACKGROUND

The Shear Lag Effect

The shear lag effect is the nonuniform stress distribution that occurs in a tension member adjacent to a connection. The total shear lag effect is a combination of both in-plane effects and out-of-plane effects. The in-plane shear lag effect is a function of the connection length and width of the connected element, while the out-of-plane effect occurs when not all of the elements of a cross section are directly connected, such as when an angle is used as a tension member and only one leg of the angle is connected, as shown in Figure 2. Eccentrically loaded members will experience a nonuniform stress distribution across the width of the member. Shear stresses acting in the plane of the member transmit stress from the location of the applied load to locations distant from the load (Salmon et al., 2009). The shear transfer "lags" behind at locations farther away from the applied load (Salmon et al., 2009). As a result of the shear lag effect, the design strength of the member must be reduced (Easterling and Giroux-Gonzalez, 1993). The shear lag factor, U, is a reduction coefficient that is multiplied by the net area to determine the effective net area for the limit state of net section fracture.

Shear lag provisions for welded members were first introduced in the *Load and Resistance Factor Design Specification for Structural Steel Buildings* (AISC, 1986) and

Case	Description of Element	Shear Lag Factor, U	Example
4[a]	Plates, angles, channels with welds at heels, tees, and W-shapes with connected elements, where the tension load is transmitted by longitudinal welds only.	$U = \dfrac{3l^2}{3l^2 + w^2}\left(1 - \dfrac{\bar{x}}{l}\right)$	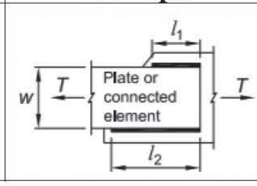

[a] $l = \dfrac{l_1 + l_2}{2}$, where l_1 and l_2 shall not be less than 4 times the weld size.

Fig. 1. AISC shear lag factor provision for Case 4 (AISC, 2016b).

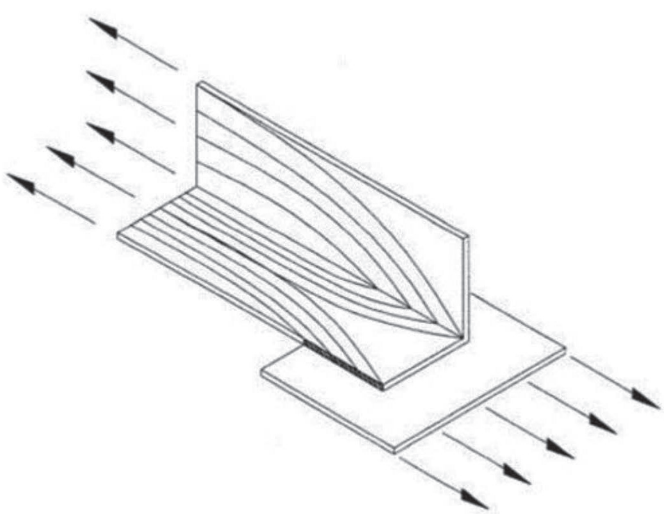

Fig. 2. Stress distribution in an angle section in tension (Mannem, 2002).

Specification for Structural Steel Buildings—Allowable Stress Design and Plastic Design (AISC, 1989). These provisions addressed only plate-type members having no eccentricity.

Shear Lag Provisions

As previously mentioned, shear lag provisions for tension members connected by longitudinal welds first appeared in the AISC *Load and Resistance Factor Design Specification for Structural Steel Buildings* (AISC, 1986). Determination of the shear lag factor for a variety of cases was tabulated in 2005 AISC *Specification* Table D3.1 (AISC, 2005), with Case 2 addressing out-of-plane eccentricity and Case 4 addressing the shear lag factor for flat plates where the tension load is transmitted by longitudinal welds only. The shear lag provisions for Case 2 and Case 4 in the subsequent 2010 AISC *Specification* (AISC, 2010), as shown in Figure 3, were virtually identical to the 2005 *Specification*.

A task group was assigned by the AISC Committee on Specifications to evaluate Table D3.1 of the AISC *Specification* (Fortney and Thornton, 2012). Fortney and Thornton described four limitations in Case 4:

1. Only plates are considered.
2. Both edges of the plate must be welded.
3. The welds must be of equal length.
4. The length of the welds, or the average thereof, must be equal to or greater than the distance between them.

During their review of Case 4, Fortney and Thornton (2012) evaluated a generalized procedure for calculating the shear lag factor in connections using longitudinal welds that included not only plate-type tension members, but also those consisting of angles, channels, and WT sections.

Fortney and Thornton (2012) reviewed past experimental research in order to investigate shear lag effects. Three experimental research programs, consisting of 175 longitudinally welded tension members, were evaluated in their study. The dataset used consisted of 158 flat plates with equal weld lengths; 4 single angles with unequal but balanced weld lengths; and 13 other members, including double angles, tees, and channels having equal weld lengths. One of the major findings was that a larger strength reduction existed in experimental data compared to the calculated value using the 2010 AISC *Specification*. They concluded that this might be a result of the in-plane shear lag effect due to the connection length not being considered in members with eccentricity. As a result, two recommendations were proposed that take into account both in-plane and out-of-plane effects to accurately predict the shear lag factor. The first recommendation, the bi-planar model, uses the product of the out-of-plane effect and the in-plane effect of Table D3.1 for the calculation of the shear lag factor (Figure 4).

In Fortney and Thornton's second recommendation, the out-of-plane effect is accounted for by using Case 2 of AISC *Specification* Table D3.1 (AISC, 2010), while the in-plane effect is accounted for by a fixed-fixed beam model. The moment-axial interaction equation of AISC *Specification* Section H1.1 (AISC, 2010) was used along with the assumption of a fixed-fixed beam with a uniformly distributed load along its length and plastic hinges forming at locations of maximum positive and negative moments. Using the conservative approximation of $F_u/F_y = 1.5$, the in-plane shear lag effect for the connected element in the second recommendation is shown in Equation 4. Figure 5 details this recommendation for Case 4 proposed by Fortney and Thornton (2012), which was incorporated in equivalent form into the 2016 *Specification*.

$$U_{CE} = \frac{1}{1+\left(\frac{1}{3}\right)\left(\frac{w}{l}\right)^2} \tag{4}$$

Case	Description of Element	Shear Lag Factor, U	Example
2	All tension members, except plates and HSS, where the tension load is transmitted to some but not all of the cross sectional elements by fasteners or longitudinal welds or by longitudinal welds in combination with transverse welds.	$U = 1 - \frac{\bar{x}}{l}$	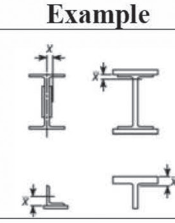
4	Plates where the tension load is transmitted by longitudinal welds only.	$l \geq 2w$ .... $U = 1.0$ $2w > l \geq 1.5w$ .... $U = 0.87$ $1.5w > l \geq w$......... $U = 0.75$	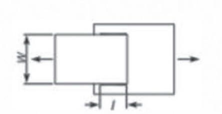

Fig. 3. 2010 AISC shear lag factor provision for welded tension members (AISC, 2010).

where

U_{CE} = shear lag factor of the connected element

l = length of the weld, in.

w = width of the plate/element, in.

The fixed-fixed beam model developed by Fortney and Thornton (2012) is now used in 2016 AISC *Specification* Table D3.1, Case 4. The current Case 4 shear lag factor removes previous limitations by accommodating weld lengths shorter than the width of the member, conditions using unequal weld lengths, and members besides flat plates.

EXPERIMENTAL PROGRAM

Research was conducted at the University of Cincinnati to study the influence of both in-plane and out-of-plane eccentricity on shear lag. The project consisted of the experimental testing of 20 longitudinally welded tension specimens consisting of eight 3×½ plates and twelve 3×3×½ angles. The specimens were ordered as ASTM A36 material and were designed assuming a yielding strength of 50 ksi and an ultimate strength of 70 ksi. The main parameters that were varied included the length of the connection and the weld configuration. Material testing was also performed to determine the actual yield and ultimate stresses of the material. Shear lag factors resulting from these tests were evaluated for their conformance to theoretical values given by 2016 AISC *Specification* Table D3.1, Case 4. The experimental shear lag factors resulting from these 20 tests were also compared to the AISC bi-planar model from Fortney and Thornton (2012), as well as the theoretical shear lag values from Case 4 in the 2010 AISC *Specification* (AISC, 2010).

Description of the Tensile Specimens

Eight 3×½ plate specimens and twelve 3×3×½ angle specimens were tested using a Tinius Olsen testing machine with a capacity of 400 kips. The configuration details of the plate specimens (Group A) and the angle specimens (Group C) are shown in Figures 6 and 7 as well as Tables 1 and 2, respectively. The clear length of all specimens was 36 in. The joint at gusset plate #1 was designed to fail, while the joint at gusset plate 2 was intended to be stronger than the connected members. Specimen C-11 was originally detailed with a transverse weld at gusset #1 (L_B = 3 in.) but the specimen was fabricated without the transverse weld. As a result, Specimen C-11 was identical to Specimen C-6.

The universal testing machine used a displacement-controlled loading at a rate of 0.125 in./min. until the yield plateau was observed. After a couple tenths of an in. of displacement in the yield plateau, the rate of loading was increased to 0.25 in./min. Each specimen was tested until failure. The experimental setup is shown in Figure 8. Each

Case	Description of Element	Shear Lag Factor, U	Example
4[a]	Plates, angles, channels, tees, and W-shapes with connected elements where the tension load is trans-mitted by longitudinal welds only.	$U = U_{CE}\left(1-\frac{\bar{x}}{l}\right)$ $l \ge 2w$ .... $U_{CE} = 1.0$ $2w > l \ge 1.5w$ .... $U_{CE} = 0.87$ $1.5w > l \ge w$......... $U_{CE} = 0.75$ $w > l$ .... $U_{CE} = 0.75(l/w)$	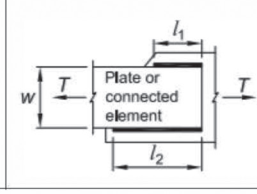

[a] $l = \frac{l_1 + l_2}{2}$, where l_1 and l_2 shall not be less than 4 times the weld size.

Fig. 4. Fortney and Thornton's (2012) bi-planar model—first recommendation.

Case	Description of Element	Shear Lag Factor, U	Example
4[a]	Plates, angles, channels, tees, and W-shapes with connected elements where the tension load is trans-mitted by longitudinal welds only.	$U = U_{CE}\left(1-\frac{\bar{x}}{l}\right)$ $U_{CE} = \frac{1}{1+\left(\frac{1}{3}\right)\left(\frac{w}{l}\right)^2}$	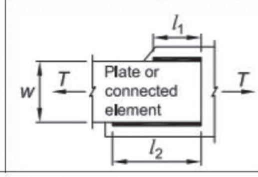

[a] $l = \frac{l_1 + l_2}{2}$, where l_1 and l_2 shall not be less than 4 times the weld size.

Fig. 5. Fortney and Thornton's (2012) fixed-fixed beam model—second recommendation.

Table 1. Group A Plate Specimen Details								
Specimen	w_1	L_A	L_B	L_C	w_2	L_D	L_E	L_F
PL3×½	(in.)	(in.)	(in.)	(in.)	(in)	(in.)	(in.)	(in.)
A-1	5⁄16	8	0	8	5⁄16	10	0	10
A-2a	5⁄16	6	0	6	5⁄16	8	0	8
A-2b	7⁄16	6	0	6	5⁄16	8	0	8
A-3	3⁄8	4	0	4	5⁄16	6	0	6
A-4	7⁄16	2	0	2	5⁄16	4	0	4
A-5	5⁄16	4	0	8	5⁄16	10	0	10
A-6	3⁄8	3	0	6	5⁄16	8	0	8
A-7	7⁄16	2	0	4	5⁄16	6	0	6

specimen was installed into the universal testing machine with the end expected to fail (i.e., gusset 1) at the bottom. Both gusset plates were gripped at their ends using mechanical grips, and shims were used in order to align the centroid of the member with the applied load. Two linear variable differential transformers (LVDTs) were attached to a plate and clamped to the specimen above and below the bottom welded connection. Also, an aluminum angle was clamped to the specimen below the top gusset plate. Monofilament was used to suspend the rods of the LVDTs from hooks attached to the aluminum angle. Rubber pads were used between the clamps and the specimen to ensure the clamps would stay snug despite the specimen becoming thinner due to Poisson effects. Load and displacement data was collected by a National Instruments data acquisition system and exported to Excel. Displacement data was also collected by the LVDTs in order to determine the elongation of the bottom welded connection. The average displacement of the top two LVDTs was subtracted from the average displacement of the bottom two LVDTs in order to determine the connection elongation. The maximum load for each specimen was found and used for the shear lag analysis.

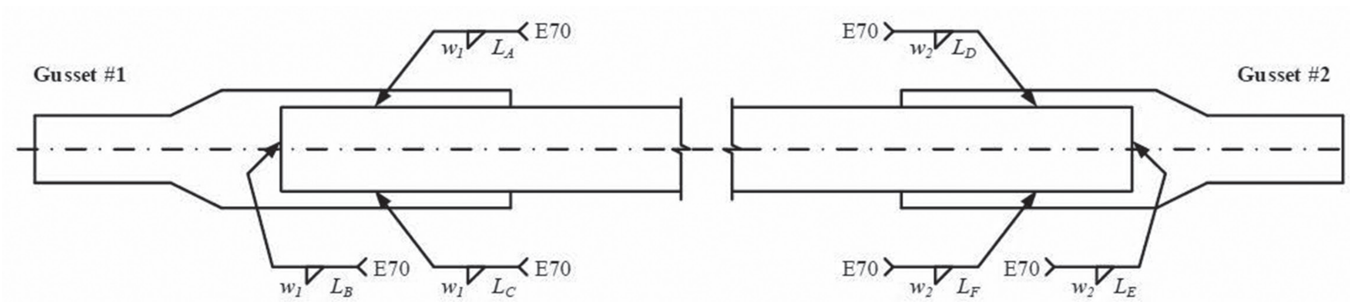

Fig. 6. Group A plate specimen.

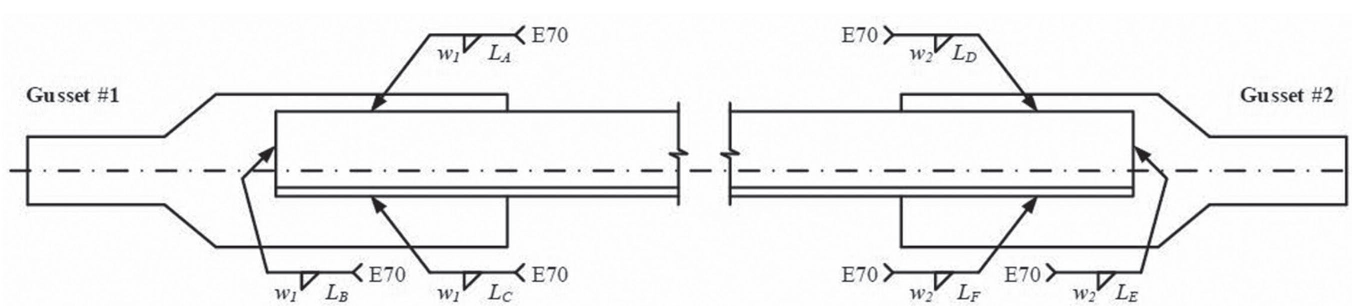

Fig. 7. Group C angle specimen.

Table 2. Group C Angle Specimen Details								
Specimen	w_1	L_A	L_B	L_C	w_2	L_D	L_E	L_F
L3×3×½	**(in.)**	**(in.)**	**(in.)**	**(in.)**	**(in)**	**(in.)**	**(in.)**	**(in.)**
C-1	3/8	8	0	8	5/16	10	0	10
C-2	7/16	6	0	6	5/16	10	0	10
C-3	7/16	4	0	4	5/16	10	0	10
C-4	7/16	2	0	2	5/16	6	0	6
C-5	7/16	4	0	8	5/16	10	0	10
C-6	7/16	3	0	6	5/16	8	3	8
C-7a	7/16	1.5	0	3	5/16	5	3	5
C-7b	7/16	1.5	0	3	5/16	5	3	5
C-8	7/16	3	0	1.5	5/16	5	3	5
C-9	7/16	6	0	3	5/16	8	3	8
C-10	7/16	8	0	4	5/16	10	0	10
C-11	7/16	3	0	6	5/16	8	3	8

Material Testing

Two steel coupons were machined and tested for both the plate and angle material provided by the fabricator. The plate and angle material coupons are designated with the letters A and C, respectively. The actual measured yield and ultimate stresses for both the plate and angle material are shown in Table 3. Note that the measured ultimate strength reached values well above 70 ksi.

EXPERIMENTAL RESULTS

The 20 longitudinally welded tension specimens experienced one of three different failure modes—a gross section failure (GSF), a net section failure (NSF), or a weld failure (WF), as shown in Table 4. Pictures of a typical failure for each mode are shown in Figures 9, 10, and 11. The specimens were originally detailed such that the welds would be stronger than the members. Despite the fact that

Fig. 8. Experimental setup of tension specimen.

Table 3. Results of Material Testing										
	Yield		Ultimate				Yield		Ultimate	
Coupon	Load	Stress	Load	Stress		Coupon	Load	Stress	Load	Stress
	(kips)	(ksi)	(kips)	(ksi)			(kips)	(ksi)	(kips)	(ksi)
A-1	10.38	53.47	15.03	77.43		C-1	10.14	51.80	14.58	74.52
A-2	10.35	53.35	15.02	77.44		C-2	10.08	51.92	14.49	74.67
Avg.	10.37	53.41	15.03	77.44		Avg.	10.11	51.86	14.54	74.60

Fig. 9. Typical gross section fracture.

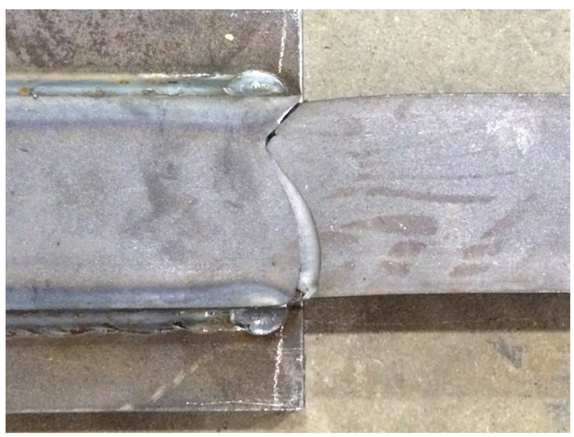

Fig. 10. Typical net section fracture.

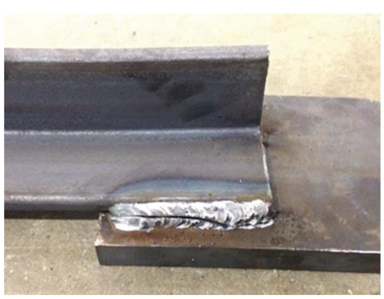

(a)

(b)

Fig. 11. Typical weld failures.

Table 4. Experimental Results						
Specimen	Failure Mode	A_g	F_y	F_u	Max Load	Experimental Shear Lag Factor, U_e
		(in.^{2})	(ksi)	(ksi)	(kips)	
A-1	GSF	1.50	53.4	77.4	111	0.96
A-2a	GSF	1.50	53.4	77.4	107	0.92
A-2b	GSF	1.50	53.4	77.4	107	0.92
A-3	GSF	1.50	53.4	77.4	107	0.92
A-4	WF	1.50	53.4	77.4	72.4	> 0.62
A-5	GSF	1.50	53.4	77.4	111	0.96
A-6	NSF	1.50	53.4	77.4	111	0.95
A-7	WF	1.50	53.4	77.4	102	> 0.87
C-1	NSF	2.76	51.9	74.6	196	0.95
C-2	WF	2.76	51.9	74.6	181	> 0.88
C-3	WF	2.76	51.9	74.6	115	> 0.56
C-4	WF	2.76	51.9	74.6	73.6	> 0.36
C-5	NSF	2.76	51.9	74.6	187	0.91
C-6	WF	2.76	51.9	74.6	156	> 0.76
C-7a	WF	2.76	51.9	74.6	86.5	> 0.42
C-7b	WF	2.76	51.9	74.6	90.3	> 0.44
C-8	WF	2.76	51.9	74.6	83.6	> 0.41
C-9	WF	2.76	51.9	74.6	127	> 0.62
C-10	WF	2.76	51.9	74.6	179	> 0.87
C-11	WF	2.76	51.9	74.6	157	> 0.76

expected material strengths, $R_yF_y = (1.5)(36) = 54$ ksi and $R_tF_u = (1.2)(58) = 70$ ksi, consistent with the AISC *Seismic Provisions* (2016a), were used for the members in the design calculations, two of the plate specimens and all but two of the angle specimens exhibited failures in the welds instead of in the member because of, at least in part, unexpectedly high strengths of the member materials. This is a consequence of the constraints dictated by the specimens' configurations, which were chosen purposely to have relatively short welds, for which the maximum weld size was limited to 7⁄16 in. and for which selecting an electrode stronger than E70 would have led to the strength of the adjacent base metal to govern, even when expected material strengths were considered. Thus, the weld strength and base metal strength were in many instances very close to each other, such that even a moderate overstrength of the base metal would force a limit state in the weld. As shown in Table 3, the measured F_u is on average 77 ksi for the plates and 75 ksi for the angles.

The maximum load for each specimen was recorded, and the experimental shear lag factors, U_e, were calculated as the ratio of the maximum load to the rupture strength (gross area × ultimate tensile stress, F_u). The ultimate tensile stress was taken as the value determined from the material coupon testing. The experimental shear lag factor for each specimen is shown in Table 4. For the specimens that did not experience net section fracture, the experimental shear lag factor can be taken to be at least equal to those shown in Table 4.

Plate Specimens

All of the experimental shear lag factors for the plate specimens, except Specimens A-4 and A-7, were greater than 0.90. This agrees with what previous researchers have found (Easterling and Giroux-Gonzalez, 1993). Specimens A-4 and A-7 both experienced weld failures; therefore, the experimental shear lag factor would have been greater than the recorded value if the welded connection had sufficient strength. To validate the consistency of the experiment, two identical specimens were tested. The results from Specimens A-2a and A-2b show the testing was very consistent because both specimens failed by gross section fracture with virtually no difference in the maximum load. To investigate the degree to which the connection length affects the experimental shear lag factor, the results from Specimens A-1 and A-3 can be compared. Specimen A-1 had two 8-in. welds with U_e = 0.96, while Specimen A-3 had two 4-in. welds with U_e = 0.92. From these results, the connection length for plates with a balanced weld configuration appears to have a minimal effect on the experimental shear lag factor, which was previously noted in a thesis by Dhungana (2014). A comparison of Specimens A-1 and A-5 reveals the effect of the weld configuration. Specimen A-1 had a balanced weld configuration with two 8-in. longitudinal welds, and Specimen A-5 had an unbalanced weld configuration with L_A = 4 in. and L_C = 8 in. Both of these specimens experienced gross section fracture and had an experimental shear lag factor of 0.96. An unbalanced weld configuration leading to in-plane eccentricity appears to have had no effect on the efficiency of longitudinally welded plates. Further review of all plate-type tension members that failed by either gross or net section failure (A-1, A-2a, A-2b, A-3, A-5, and A-6) also supports the premise that in-plane eccentricity appeared to have little effect on the experimental shear lag factor, U_e. The four plate specimens with balanced weld configurations (A-1, A-2a, A-2b, and A-3) had shear lag factors that ranged between 0.92 and 0.96, while the two plate specimens with unbalanced weld configurations (A-5 and A-6) had shear lag factors of 0.96 and 0.95, respectively.

Angle Specimens

The experimental shear lag factors, U_e, for two angle specimens (C-1 and C-5) that failed by net section fracture were 0.95 and 0.91, respectively. For the angles experiencing weld failures, the experimental shear lag factors ranged from 0.36 to 0.88. Larger values for these experimental shear lag factors would have been achieved if the welded connection had sufficient strength to reach the net section capacity of these members. To confirm consistency in testing of the angles, two identical specimens were tested. The results from Specimens C-7a and C-7b show the testing was again very consistent from specimen to specimen. Both members failed through the weld with a slight difference in the maximum load. Specimens C-1 (unbalanced weld configuration) and C-5 (balanced weld configuration) did experience net section failure while the remaining angle specimens experienced weld failure. Although only two specimens experienced net section failure, the experimental shear lag factor, U_e, of both Specimens C-1 and C-5 exceeded the theoretical shear lag factor, U_t, of the 2016 *Specification*.

The angles that experienced net section fracture (C-1 and C-5) were compared with plate specimens (A-1 and A-5) that had similar weld configurations at each end. The plates experienced gross section fracture and failed as designed at the bottom, with Specimen A-1 having a balanced connection and Specimen A-5 having an unbalanced connection. Both angles, however, failed at the top connection under a combination of in-plane and out-of-plane eccentricity. The experimental shear lag factor, U_e, was 0.95 for angle Specimen C-1 and 0.91 for angle Specimen C-5 as compared to 0.96 for the plates.

DISCUSSION

Theoretical Shear Lag Factors

Theoretical shear lag factors, U_t, were calculated using the 2010 AISC *Specification* (AISC, 2010), the bi-planar model from Fortney and Thornton (2012), and the 2016 AISC *Specification* (AISC, 2016b). The theoretical shear lag factors for the AISC bi-planar model and those using the 2010 AISC *Specification* were calculated based on the requirements developed by Fortney and Thornton and the 2010 AISC *Specification*, respectively. The theoretical shear lag factors based on the 2016 AISC *Specification* were calculated using Table D3.1, Case 4, for the angle and plate specimens. These values are shown in Table 5 along with the ratio of experimental to theoretical shear lag factors, U_e/U_t.

Using the 2010 AISC *Specification*, the values of U_e/U_t for the plate specimens ranged from 0.92 to 1.23, with two values greater than or equal to 1.00. For the angle specimens, U_e/U_t ranged from 0.67 to 1.08, with eight values being lower than 1.00. All of the U_e/U_t values less than 1.00 for the angle specimens experienced weld failure.

Using the bi-planar model (Fortney and Thornton, 2012), the values of U_e/U_t for the plate specimens ranged from 0.92 to 1.24 with three of the eight members having values equal to or greater than 1.00. These values were the same as those for the aforementioned 2010 AISC *Specification* values with the exception of the value of U_e/U_t for Specimen A-4, which was not calculated because the 2010 AISC *Specification* did not allow l/w to be less than 1.0. For the 12 angle specimens, U_e/U_t ranged from 0.90 to 1.33, with only two values less than 1.00. These two values were from specimens that experienced weld failure.

Using the 2016 AISC *Specification*, the values of U_e/U_t for the plate specimens ranged from 0.99 to 1.16, with seven of the eight members having values equal to or greater than 1.0. The one plate member (A-6) failing at the net section had a theoretical shear lag virtually equal to the experimental value. For the angle specimens, the values ranged from 0.87 to 1.19, with only two values being less than 1.00. The two values that were less than 1.00 were for members (C-3 and C-9) that failed through the weld, indicating that the experimental shear lag value for these members would have been higher had they been able to reach net section capacity before the welds failed.

Table 5. Experimental and Theoretical Shear Lag Factors

Specimen	Experimental Shear Lag Factor, U_e		$\frac{l}{w}$	Theoretical Shear Lag Coefficient, U_t			$\frac{U_e}{U_t}$		
				2010	Bi-Planar	2016	2010	Bi-Planar	2016
A-1	0.96		2.67	1.00	1.00	0.96	0.96	0.96	1.00
A-2a	0.92		2.00	1.00	1.00	0.92	0.92	0.92	1.00
A-2b	0.92		2.00	1.00	1.00	0.92	0.92	0.92	1.00
A-3	0.92		1.33	0.75	0.75	0.84	1.23	1.23	1.10
A-4	> 0.62		0.67	*	0.50	0.57	*	>1.24	>1.09
A-5	0.96		2.00	1.00	1.00	0.92	0.96	0.96	1.04
A-6	Top connection	0.95	2.67	1.00	1.00	0.96	0.95	0.95	0.99
	Bottom connection	>0.95	1.50	0.87	0.87	0.87	>1.09	>1.09	>1.09
A-7	>0.87		1.00	0.75	0.75	0.75	>1.16	>1.16	>1.16
C-1	Top connection	0.95	3.33	0.91	0.91	0.88	1.04	1.04	1.08
	Bottom connection	>0.95	2.67	0.88	0.88	0.84	>1.08	>1.08	>1.13
C-2	> 0.88		2.00	0.85	0.85	0.78	>1.04	>1.04	>1.13
C-3	> 0.56		1.33	0.77	0.58	0.65	>0.73	>0.97	>0.87
C-4	> 0.36		0.67	0.54	0.27	0.31	>0.67	>1.33	>1.18
C-5	Top connection	0.91	3.33	0.91	0.91	0.88	1.00	1.00	1.03
	Bottom connection	>0.91	2.00	0.85	0.85	0.78	>1.08	>1.07	>1.17
C-6	> 0.76		1.50	0.79	0.69	0.69	>0.96	>1.10	>1.10
C-7a	> 0.42		0.75	0.59	0.33	0.37	>0.72	>1.27	>1.14
C-7b	> 0.44		0.75	0.59	0.33	0.37	>0.75	>1.33	>1.19
C-8	> 0.41		0.75	0.59	0.33	0.37	>0.70	>1.24	>1.11
C-9	> 0.62		1.50	0.79	0.69	0.69	>0.78	>0.90	>0.90
C-10	> 0.87		2.00	0.85	0.85	0.78	>1.03	>1.02	>1.12
C-11	> 0.76		1.50	0.79	0.69	0.69	>0.96	>1.10	>1.10

* 2010 AISC *Specification* did not allow $l/w < 1$.

A comparative analysis of the U_e/U_t ratios based on the three methods was performed. In order for the theoretical shear lag factor to be conservative, the ratio U_e/U_t needs to be greater than or equal to 1.00. Figure 12 shows a comparison of the U_e/U_t ratio for the 20 specimens tested using the three aforementioned methods of determining theoretical shear lag factors. The 2016 AISC *Specification* based on the fixed-fixed beam model performed best, with 85% of the members tested (17 of the 20) having a U_e/U_t ratio exceeding 1.00. In addition to the high percentage of tests having a U_e/U_t ratio exceeding 1.00, the 2016 AISC *Specification* for shear lag also shows much less variability than either of the other two methods used in this comparison. The bi-planar model had 65% of the members tested (13 of the 20) with a U_e/U_t ratio exceeding 1.00, while the 2010 AISC *Specification* was the least conservative because only 32% of the members tested (6 of the 19) had a U_e/U_t ratio exceeding 1.00. In addition, the comparison showed that U_e/U_t values for both the bi-planar model and the 2010 AISC *Specification* were more variable than those using the 2016 AISC *Specification*.

Another comparison was performed based on the average length of the welds versus the distance between the welds, l/w. Graphs of shear lag factor versus l/w are presented in Figures 13, 14, and 15. After comparing the experimental shear lag factors of the 20 welded specimens to the theoretical values from the three methods, it can be seen that the experimental shear lag factors for members experiencing non-weld failure conform closely to provisions given in 2016 *Specification* Table D3.1, Case 4. For the five plates that experienced either gross or net section failure the U_e/U_t

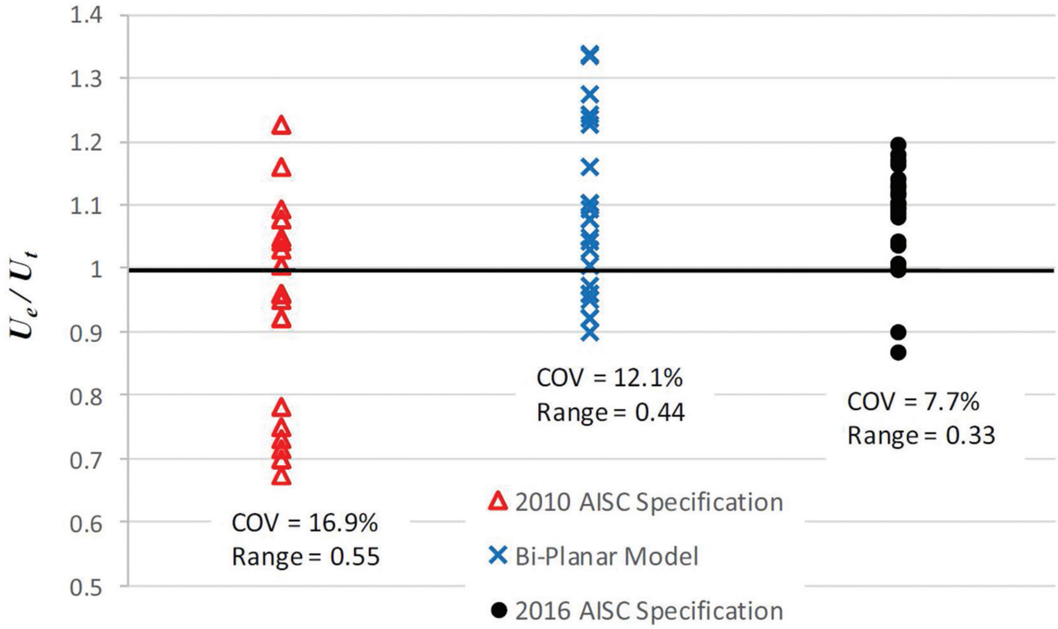

Fig. 12. U_e/U_t *Comparison between different shear lag models.*

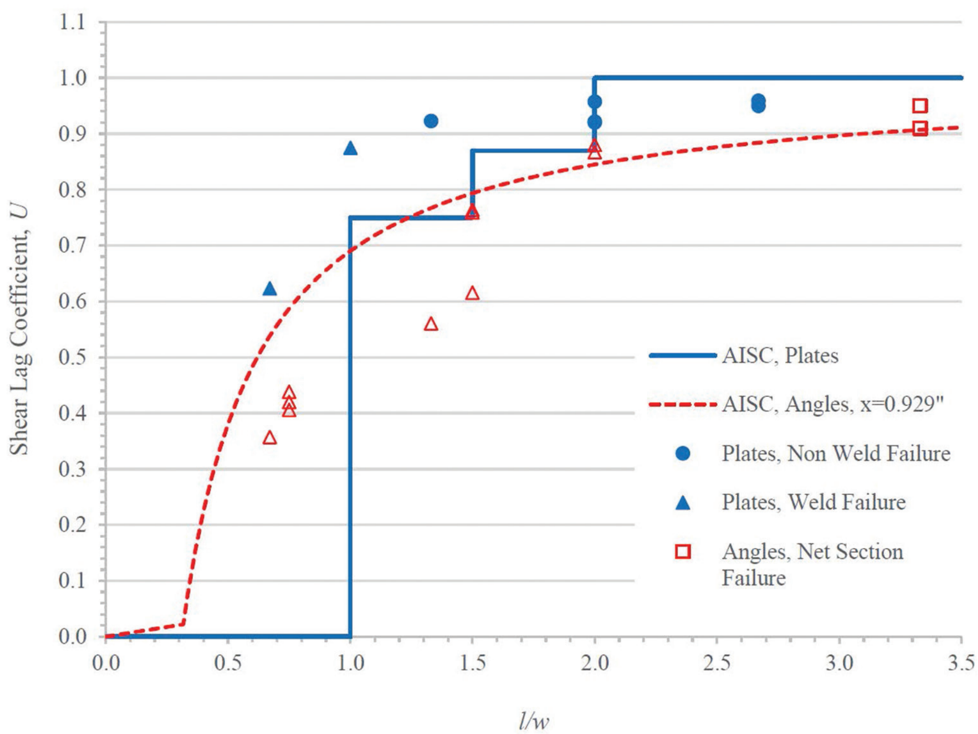

Fig. 13. Shear lag factor versus l/w *using the 2010 AISC* Specification.

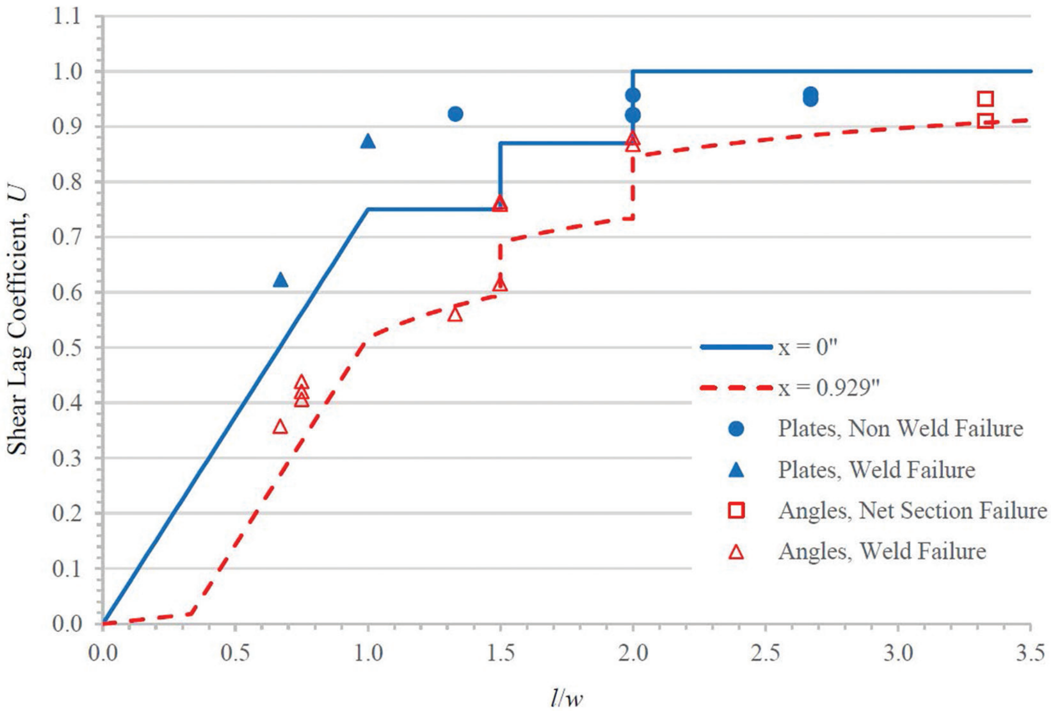

Fig. 14. Shear lag factor versus l/w *using Fortney and Thornton's (2012) bi-planar recommendation.*

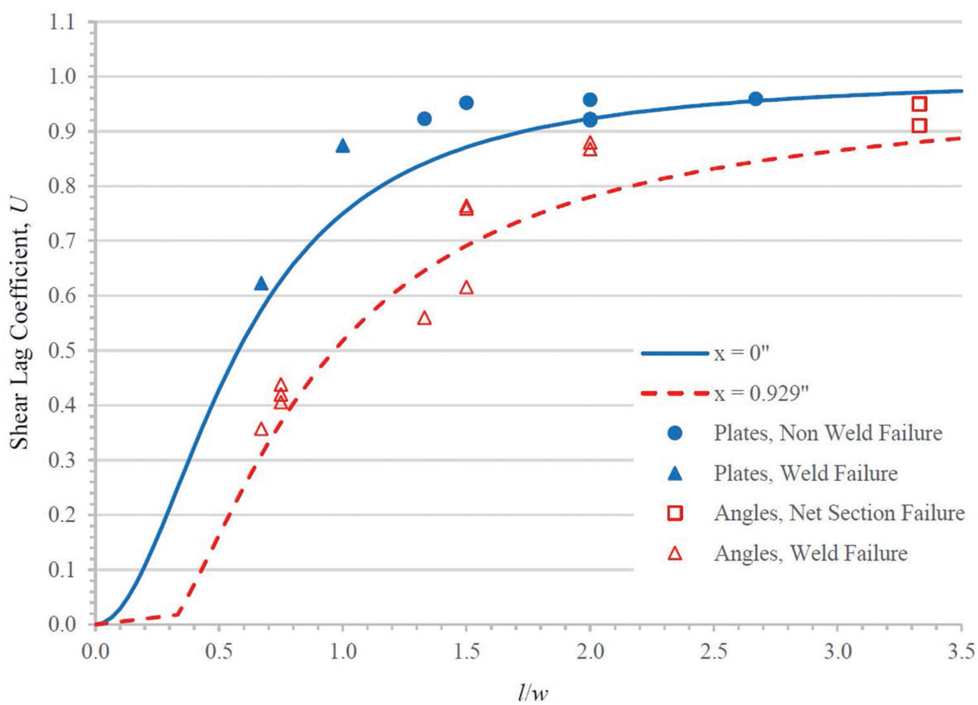

Fig. 15. Shear lag factor versus l/w *using the 2016 AISC* Specification.

ratio ranged from 0.99 to 1.10, with l/w ratios that varied between 1.33 and 2.67. Although only two angles experienced net section failure, those two members had a U_e/U_t ratio ranging from 1.03 to 1.08, and each angle had an l/w ratio of 3.33. This indicates that Case 4 from the 2016 AISC *Specification* seems to adequately predict shear lag factor over a wide range of l/w ratios.

Another item of note is the behavior of the experimental specimens with a length-to-width ratio under 1.0 (i.e., $l/w < 1.0$). The 2016 AISC *Specification* removed the previous limitation that the length of the longitudinal welds must be greater than or equal to the distance between them. The experimental results discussed herein contained four angles and one plate with l/w ratios of less than 1.0. Although, perhaps not surprisingly, all five of these tension members experienced weld failures, the U_e/U_t ratio for these specimens ranged from 1.09 to 1.19 when compared to the 2016 *Specification*. When the U_e/U_t ratio for these five members was calculated using the bi-planar model (Fortney and Thornton, 2012) the range is 1.24 to 1.33. This suggests that the experimental specimens with $l/w < 1.0$ appear to conform most closely with the 2016 AISC *Specification*.

SUMMARY AND CONCLUSIONS

The main objective of this paper was to experimentally test 20 longitudinally welded tension specimens and compare the experimental shear lag factor to theoretical values from three methods. Eight 3×½ plate sections and twelve 3×3×½ angle sections were tested. The parameters that were varied include the length of the connection and the weld configuration. Also, four coupons—two from the plate material and two from the angle material—were tested in tension to determine the yield stress and the ultimate stress of the plate and angle material.

The experimental shear lag factor, U_e, for each specimen was calculated as the ratio of the maximum load measured to the rupture strength. Experimental shear lag factors were determined for each of the 20 tested specimens and compared to three theoretical values: (1) the shear lag factor from Case 4 in the 2016 AISC *Specification*, (2) the shear lag factor based on a bi-planar model (Fortney and Thornton, 2012), and (3) the shear lag factor from the 2010 AISC *Specification*. The ratio of the experimental shear lag factor to the theoretical, U_e/U_t, was used to identify which of the three methods provided the best prediction of shear lag behavior. Trends of the experimental shear lag factor were also studied with respect to the influence of connection length versus width, l/w.

Based on the results from the experimental program and a comparison of shear lag factors to the aforementioned provisions, it has been found that:

2016 AISC *Specification* Table D3.1, Case 4, provides the best prediction of shear lag factor in longitudinally welded tension members under the influence of eccentricity. The 20 tension members tested in this experiment, with a mixture of balanced and unbalanced longitudinal welds, showed that shear lag factors using the 2016 AISC *Specification* had the highest percentage of U_e/U_t ratios at or above 1.0 with the least variation as compared to the 2010 AISC *Specification* as well as to the bi-planar model studied by Fortney and Thornton.

2016 AISC *Specification* Table D3.1, Case 4, provides the best prediction of shear lag factor in longitudinally welded tension members with connection length-to-width ratios of less than 1.0 ($l/w < 1.0$). The experimental tension members with $l/w < 1.0$ conformed more closely to the 2016 AISC *Specification* than to the bi-planar model. For members with $l/w < 1.0$ using the AISC bi-planar model, the U_e/U_t ratio ranged from 1.24 to 1.33 while the same value ranged from 1.09 to 1.19 using the 2016 AISC *Specification*.

For the flat plate specimens, all of the experimental shear lag factors were greater than 0.90, except for the two specimens that failed via weld fracture. The connection length for plates with a balanced weld configuration appears to have had a small effect on the experimental shear lag factor. The testing of a specimen having two 8-in. welds resulted in an experimental shear lag factor of 0.96, while a similar tension member having two 4-in. welds resulted in an experimental shear lag factor of 0.92. This difference is less than that predicted by the 2016 AISC *Specification*.

For the flat plate specimens, the presence of in-plane eccentricity appeared to have had little effect on the experimental shear lag factor, U_e. Among plates that experienced gross or net section failure, the four plate specimens with balanced weld configurations had shear lag factors that ranged between 0.92 and 0.96, while the two plate specimens with unbalanced weld configurations had shear lag factors of 0.96 and 0.95, respectively. A comparison of the experimental shear lag factor for these six specimens conformed very closely with the theoretical shear lag factor based on the 2016 AISC *Specification*.

ACKNOWLEDGMENTS

The authors gratefully acknowledge Mr. Gregory Lynch, with Almet Inc. of New Haven, Indiana, for the fabrication of the specimens that were part of this testing program.

REFERENCES

AISC (1986), *Load and Resistance Factor Design Specification for Structural Steel Buildings*, American Institute of Steel Construction, Chicago, Ill.

AISC (1989), *Specification for Structural Steel Buildings—Allowable Stress Design and Plastic Design*, American Institute of Steel Construction, Chicago, Ill.

AISC (2005), *Specification for Structural Steel Buildings*, ANSI/AISC 360-05, American Institute of Steel Construction, Chicago, Ill.

AISC (2010), *Specification for Structural Steel Buildings*, ANSI/AISC 360-10, American Institute of Steel Construction, Chicago, Ill.

AISC (2016a), *Seismic Provisions for Structural Steel Buildings*, ANSI/AISC 341-16, American Institute of Steel Construction, Chicago, Ill.

AISC (2016b), *Specification for Structural Steel Buildings*, ANSI/AISC 360-16, American Institute of Steel Construction, Chicago, Ill.

Dhungana, U. (2014), *Shear Lag Factor for Longitudinally Welded Tension Members Using Finite Element Method*, Thesis, University of Cincinnati, Cincinnati, Ohio.

Easterling, W.S. and Giroux-Gonzalez, L. (1993), "Shear Lag Effects in Steel Tension Members," *Engineering Journal,* AISC, Vol. 30, No. 3, pp. 77–88.

Fortney, P.J. and Thornton, W.A. (2012), "Recommendations for Shear Lag Factors for Longitudinally Welded Tension Members," *Engineering Journal,* AISC, Vol. 49, No. 1, pp. 11–32.

Mannem, R. (2002), *Shear Lag Effects on Welded Steel Angles and Plates*, Thesis, Department of Civil Engineering, University of Newfoundland.

Salmon, C.G., Johnson, J.E., and Malhas, F.A. (2009), *Steel Structures: Design and Behavior*, Pearson Education Inc., Upper Saddle River, N.J.